



Effect of linewidth enhancement factor of laser diode and fiber dispersion management on high-speed optical fiber links performance and use in WDM systems

Alaa Mahmoud¹ · Nada Fouad¹ · Moustafa Ahmed^{2,3} · Tarek Mohamed¹

Received: 8 June 2022 / Accepted: 7 November 2022 / Published online: 3 January 2023
© The Author(s) 2022

Abstract

We present a numerical simulation study on the effect of the linewidth enhancement factor (α) of semiconductor laser and dispersion management methods of optical fibers on the performance of 40-Gb/s directly-modulated fiber links and their application in WDM systems. The dispersion management methods include the use of non-zero dispersion-shifted fiber (NZ-DSF), dispersion-compensating fiber (DCF), and fiber Bragg grating (FBG). The optimal values of the α -parameter and the best dispersion management method are applied to design and simulate a four-channel \times 40-Gb/s WDM fiber system. The obtained results show that the increase in the α -parameter and/or fiber length reduces the performance of both the 40-Gb/s optical link and the WDM system. Regarding the 40-Gb/s optical link, when $\alpha = 1$, using $-$ NZ-DSF or $+$ NZ-DSF, DCF with SSMF, and FBG with SSMF work to increase the transmission length from 1.6 km of a standard single-mode fiber (SSMF) to 7.2, 26.5, and 40 km, respectively. Whereas at $\alpha = 3.5$, the maximum transmission length reaches 1.2 km when using SSMF, $-$ NZ-DSF, or $+$ NZ-DSF, while it increases to 13 and 35 km when using DCF with SSMF, and FBG with SSMF, respectively. In the designed WDM system, the use of FBG with SSMF is predicted as the most effective method for dispersion management. The maximum transmission length reaches 25 km when $\alpha = 1$, but reduces to 12 km when $\alpha = 3.5$.

Keywords Laser diode · WDM · Chromatic dispersion · Linewidth enhancement factor · NZ-DSF · DCF · FBG

✉ Alaa Mahmoud
alaa.abutaleb@lira.bsu.edu.eg

¹ Laser Institute for Research and Applications LIRA, Beni-Suef University, Beni-Suef 62511, Egypt

² Department of Physics, Faculty of Science, Minia University, El-Minia 61519, Egypt

³ Department of Physics, Faculty of Science, King Abdulaziz University, 80203, Jeddah 21589, Saudi Arabia

1 Introduction

Optical fiber links have become one of the cores of modern telecommunication networks due to their rapid development, especially with the increasing demand for high transmission speeds in recent years. Therefore, high-speed transmission systems have attracted great interest, even if they are short-range optical links (ITU-T draft recommendation G.693 2001). Moreover, wavelength division multiplexing (WDM) systems are widely used in existing communication structures to transmit several channels simultaneously over a single fiber in order to reduce the cost (Ellinas and Roudas 2012). The direct modulation of laser diodes (LDs) is preferred as a data transmission technique in WDM systems to decrease power consumption and reduce the overall system cost when compared to the external modulation technique (Agrawal 2012; Zhang et al. 2018). However, under direct intensity modulation of high-speed LDs, the changes in the carrier density injected into the active region cause simultaneous changes in the refractive index and optical gain, resulting in intensity-phase coupling (Agrawal and Dutta 1986; Agrawal 2012; Zhang et al. 2018). This adds to the broadening of the spectral lineshape by a factor of $1 + \alpha^2$, where α is the so-called “linewidth enhancement factor” (or transient chirp parameter) (Henry 1982; Osinski and Buus 1987; Agrawal and Bowden 1993). Therefore, intensive theoretical and experimental investigations have been performed on the effect of the α -parameter on laser behavior (Westbrook and Adams 1988; Chow and Depatie 1988; Agrawal 1989; Duan et al. 1990; Olofsson and Brown 1992; Yousuf 2019). The chirping effect becomes more severe for high-speed LDs due to their large differential gain (Sato et al. 2005), which is expected to limit the performance of high-speed WDM systems (Antoniades et al. 2004).

The dispersion effect of the optical fiber is another limiting factor for high-speed WDM systems. The chromatic dispersion of SSMFs interacts with the frequency chirping of the directly modulated laser signals, which adds to the pulse broadening when propagating down the fiber (Cartledge and Burley 1989; Peral et al. 1998; Agrawal 2002; del Río Campos et al. 2011). As the fiber length increases, the optical pulses overlap each other and cannot be distinguished, a phenomenon known as inter-symbol interference (Krehlik 2006; del Río Campos and Horche 2012). This causes limitations on the fiber length and the data transmission bit rate (Krehlik 2006, 2007; del Río Campos and Horche 2012; Ahmed 2012). Therefore, it is important to reduce the accumulated dispersion along the fiber in order to increase the BL-product of the fiber link. Various methods have been developed for overcoming this dispersion limitation of SSMF, and are widely used in wide area networks to improve the fiber link performance (Tomkos et al. 2001a, b; Agrawal 2002; Pande and Pal 2003; Krehlik 2007; Tan et al. 2009; Mohammadi et al. 2011; Priya et al. 2015; Kaur et al. 2015; Chaoui et al. 2015; Chakkour et al. 2017; Meena and Meena 2020). One such method is to replace SSMF with non-zero dispersion-shifted fiber (NZ-DSF), which works to minimize the effects of chromatic dispersion (Tomkos et al. 2001a, b; Krehlik 2007; Priya et al. 2015). Another method that nearly cancels the dispersion of SSMF is the use of dispersion-compensating fibers (DCFs), which are typically used after SSMF (Pande and Pal 2003; Kaur et al. 2015). Fiber Bragg gratings (FBGs) are also used to reduce the dispersion effect of SSMF. FBG is used after the SSMF and acts as an optical reflection filter that reflects the desired wavelengths of the light signal while transmitting all others (Kashyap 1999; Tan et al. 2009; Mohammadi et al. 2011; Chaoui et al. 2015; Chakkour et al. 2017; Meena and Meena 2020). Previous studies have demonstrated that the use of FBG outperforms the DCFs in reducing the SSMF dispersion effect over the long fibers (Chaoui et al. 2015; Chakkour et al. 2017; Meena and Meena 2020). The previous studies

on dispersion management were related to their effect on the performance of fiber links especially under external modulation (Mohammadi et al. 2011; Priya et al. 2015; Kaur et al. 2015; Chaoui et al. 2015; Chakkour et al. 2017; Meena and Meena 2020). However, the extension of these reports to study the use of dispersion management techniques to directly-modulated fiber networks, such as WDM systems, is lacking.

In this paper, we root to the physics of LDs and their application in fiber communication systems by introducing numerical investigations on the effect of the α -parameter on the performance of 40-Gb/s directly modulated optical fiber links subject to various dispersion management methods (NZ-DSF, DCF, and FBG). The main target is to find out the optimal values of the α -parameter and the best dispersion management method that corresponds to the best performance of a high-speed fiber link. The simulated fiber link with optimum parameters is then utilized to design and simulate a four 40-Gb/s-channel WDM system. The performance of both the optical fiber link and the WDM system is evaluated in terms of the eye diagram and Q -factor of the transmitted signal. The study is based on numerical integration of the laser rate equations and the nonlinear Schrodinger equation of signal propagation down optical fibers applying a non-return to zero (NRZ) pseudorandom bit stream in the platform of the "Optisystem" software.

The theoretical model and simulation method used in this study are given in Sect. 2. The simulation results and discussions are presented in Sect. 3, and the conclusions are listed in Sect. 4.

2 Theoretical model and simulation methodology

2.1 Dynamic behaviors of laser diode

Typically, the dynamic behavior and modulation properties of the laser diode under direct modulation are simulated by the following rate equations, which describe the time evolutions of injected carrier density $N(t)$, emitted photon density $S(t)$, and optical phase $\theta(t)$ (Cartledge and Burley 1989).

$$\frac{dN(t)}{dt} = \frac{I(t)}{qV} - \frac{v_g a_o (N(t) - N_o)}{1 + \varepsilon S(t)} S(t) - \frac{N(t)}{\tau_e} + F_N(t) \quad (1)$$

$$\frac{dS(t)}{dt} = \frac{\Gamma v_g a_o (N(t) - N_o)}{1 + \varepsilon S(t)} S(t) - \frac{S(t)}{\tau_p} + \frac{\Gamma \beta N(t)}{\tau_e} + F_S(t) \quad (2)$$

$$\frac{d\theta(t)}{dt} = 2\pi \Delta \nu(t) = \frac{\alpha}{2} [\Gamma v_g a_o (N(t) - N_o) - \frac{1}{\tau_p}] + F_\theta(t) \quad (3)$$

where $I(t)$ represents the time-varying current injected into the active region, V is the active region volume, q is the electron charge, ε is the nonlinear gain compression coefficient, which is added phenomenologically to describe the reduction in optical gain by a factor of $(1 + \varepsilon S)^{-1}$ above the threshold and at high photon densities (Nagarajan et al. 1992; Wang et al. 1993), v_g is the group velocity, a_o is the differential gain coefficient, N_o is the carrier density at transparency, τ_e and τ_p are the electron and photon lifetimes, respectively, Γ is the optical confinement factor, β is the spontaneous emission factor, which describes the

fraction of spontaneous emission coupled into the lasing mode, α is the linewidth enhancement factor, and $\Delta\nu(t)$ is the time-dependent optical frequency variation (laser frequency chirp) within the active region. $F_N(t)$, $F_S(t)$ and $F_\theta(t)$ are Langevin noise source terms that are added to take into account the quantum noises on the photon and electron densities and optical phase, respectively (Agrawal 2002). The rate Eqs. (1)–(3) are solved numerically by the fourth-order Runge–Kutta algorithm (Forsythe 1977).

In direct digital modulation of LDs, the injection current term $I(t)$ of Eq. (1) represents the stream of coded bits of the electrical signal as:

$$I(t) = I_b + I_m \Psi_m(t) \tag{4}$$

where I_b is the dc-bias current, I_m is the modulation peak current and $\Psi_m(t)$ is a time-varying function with either a "0" or "1" level that describes the modulating current bit format. The corresponding time variation of the modulated laser power $P(t)$ is given by the relationship:

$$P(t) = \frac{V\eta_o h\nu}{2\Gamma\tau_p} S(t) \tag{5}$$

where η_o is the differential quantum efficiency, ν is the optical frequency, and h is Planck’s constant. The frequency chirp can be expressed in terms of the modulated laser power as (Koch and Bowers 1984; Tucker 1985; Tomkos et al. 2001a, b):

$$\Delta\nu(t) = \frac{\alpha}{4\pi} \left\{ \frac{d}{dt} [\ln P(t)] + kP(t) \right\} \tag{6}$$

where $k = 2\Gamma\varepsilon/V\eta_o h\nu$, is the adiabatic chirp coefficient, which is determined by the laser structure (Tucker 1985). The linewidth enhancement factor α simulates the variations of the active region refractive index (n) and gain per unit length (g) with the carrier density N inside the cavity. The impact of α on the dynamical properties of the laser is described by the following equation (Henry 1982):

$$\alpha = -\frac{4\pi}{\lambda} \left(\frac{\partial n/\partial N}{\partial g/\partial N} \right) \tag{7}$$

where λ is the emitted laser wavelength ($=1.55 \mu\text{m}$ in this study). The first term of Eq. (6) represents the transient chirp, which is related to the laser relaxation oscillation overshoots; the high overshoots induce a high transient chirp (Yousuf and Najeeb-ud-din 2016). The second term in Eq. (6) represents the adiabatic chirp, which is caused by the effects of spontaneous emission and gain compression and is associated with the frequency offset between the "1" and "0" power levels during modulation (Yousuf and Najeeb-ud-din 2016).

2.2 Signal propagation down the fiber

When the electric field (E) of the modulated laser signals transmitted over SSMF is assumed to maintain its polarization along the fiber, the pulse-envelope amplitude of the filed E is expected to change slowly and delay for a time of L/v_g to arrive at the far end of the fiber, where L is the fiber length. This induces a reduced time $\tau = t - L/v_g \equiv t - \beta_1 L$, where β_1 is the first-order dispersion, and consequently the time evolution of $E(L, \tau)$ along

the fiber can be represented by the following nonlinear Schrödinger equation as (Potasek and Agrawal 1987; Agrawal 2001):

$$\frac{\partial E(L, \tau)}{\partial L} + \alpha_f E(L, \tau) + i\beta_2(\omega_o) \frac{\partial^2 E(L, \tau)}{\partial \tau^2} = 0 \quad (8)$$

where α_f is the fiber attenuation coefficient, β_2 is the group velocity dispersion (GVD) that is responsible for the pulse broadening inside the fiber, and ω_o is the reference frequency of the signal. The above equation is commonly calculated by the split-step FFT method (Potasek and Agrawal 1987; Agrawal 2001; Sinkin et al. 2003). In the current numerical integration of the nonlinear Schrodinger Eq. (8) for the current scalar case of preserving the polarization state, the step size is variable not fixed; it is adaptively changed depending on the value of the maximum (over time window) nonlinear phase shift induced by the self-phase modulation effect per step (Sinkin et al. 2003). Typically, the frequency spread ($\Delta\omega$) caused by GVD is represented by the range of wavelengths ($\Delta\lambda$) emitted by the optical source. Using $\omega = 2\pi c/\lambda$ and $\Delta\omega = (-2\pi c/\lambda^2)\Delta\lambda$, the dispersion parameter (D) is given as:

$$D = \frac{d\beta_1}{d\lambda} = \frac{d}{d\lambda} \left(\frac{1}{v_g} \right) = -\frac{2\pi c}{\lambda^2} \beta_2 \quad (9)$$

where c is the speed of light in a vacuum. It is worth mentioning that optical pulses can be affected even when $D=0$ (i.e., when λ is zero-dispersion wavelength λ_{ZD}). This is due to the higher-order dispersion effects that are defined by the so-called "dispersion slope" $S=dD/d\lambda$. The third-order dispersion leads to pulse distortion and trailing. However, the transmitted pulse in the communication is wide, so the influence of the third-order and other higher-order dispersion on pulses is very small (Agrawal 2002; Albeladi 2013).

2.3 Dispersion management methods

The first method utilized in this paper for dispersion management is to replace the SSMF with a non-zero dispersion-shifted fiber NZ-DSF (i.e. λ_{ZD} is shifted to be close to 1.55 μm). Such NZ-DSF is typically designed with a GVD parameter lower than that of SSMF ($D_{SSMF} \sim +16.75$ ps/nm/km); $D_{NZ-DSF} \approx +4.5$ ps/nm/km (known as +NZ-DSF) or ≈ -7.5 ps/nm/km (known as -NZ-DSF). These values of the dispersion parameter of NZ-DSF are specifically selected to avoid the effect of four-wave mixing (Kumano et al. 2002; Krehlik 2007; Harboe et al. 2008; Recommendation ITU-T G.655 2009).

The second method is to compensate the positive chromatic dispersion accumulated along the SSMF by using DCF, which is often placed after SSMF in the fiber link (Liu et al. 1999). The idea behind this method is that the dispersion-length product of the DCF is the additive inverse of that of SSMF, and thus the total equivalent dispersion of the optical link is reduced almost to zero (Chang et al. 1996). By assuming the modulating optical pulse to travel through two fiber segments, one is SSMF with length L_{SSMF} and dispersion D_{SSMF} and the other is DCF with length L_{DCF} and dispersion D_{DCF} , the condition for ideal dispersion compensation is given as (Lu 2002; Mohammed et al. 2014),

$$D_{SSMF}L_{SSMF} + D_{DCF}L_{DCF} = 0 \quad (10)$$

According to the standard telecommunication fibers at 1.55 μm , D_{SSMF} is a positive value (i.e. SSMFs have anomalous GVD), and hence D_{DCF} must be a negative value (i.e.

DCF must have normal GVD) (Agrawal 2002). In addition, L_{DCF} should be chosen to satisfy the condition that

$$L_{DCF} = -\frac{D_{SSMF}}{D_{DCF}}L_{SMF} \tag{11}$$

Practically, L_{DCF} is designed as small as possible with a high negative value of D_{DCF} to reduce the cost (Agrawal 2002). In this paper, D_{DCF} is set as large as -82 ps/nm/km with a small L_{DCF} to satisfy the condition of Eq. (11) (Liu et al. 1999; Hayee and Willner 1999; Grüner-Nielsen et al. 2000; Agrawal 2002).

The third method to manage the dispersion effect of SSMF is the use of FBG. FBG is a small segment of the fiber that has a periodic difference in refractive index (grating) and acts as an optical reflection filter that reflects the exact wavelength of the light signal while transmitting all others (Agrawal 2002). The optical signal propagated in FBG is reflected in the reverse direction by the grating according to the Bragg condition $\lambda_B = 2\tilde{n}\Lambda$, where λ_B is the Bragg wavelength, \tilde{n} and Λ are the effective refractive index of the fiber core and the grating period, respectively (Othonos et al. 2006; Ismail et al. 2013). In the case of chirped gratings, λ_B varies along the grating length depending on the variation of optical period $\tilde{n}\Lambda$ that can be varied by either \tilde{n} or Λ (Kashyap 1999), and hence different wavelength components of the incident optical signal are reflected at different points depending on where the Bragg condition is locally satisfied (Agrawal 2002). The physical principle underlying the use of FBG to compensate for the SSMF dispersion is explained as follows. The shorter wavelength components propagate faster than the longer-wavelength ones in SSMF at $1.55 \mu\text{m}$ (that is, anomalous GVD). This can be compensated by designing FBG that provides a normal GVD in which the shorter wavelength components are reflected slower than the longer ones (Kashyap 1999). In other words, the shorter wavelengths of SSMF are reflected from the shorter optical period $\tilde{n}\Lambda$ taking a long time, while the longer wavelengths of SSMF are reflected from the longer period taking a shorter time. Typically, the round-trip time inside the grating, which represents the group-delay time inside FBG, is given by,

$$\tau_g = \frac{2\tilde{n}L_g}{c} \tag{12}$$

where L_g is the total grating length. Assuming that the optical period changes linearly along its length, the FBG dispersion parameter (D_g) can be calculated as (Kashyap 1999; Agrawal 2002):

$$D_g = \frac{\tau_g}{L_g\Delta\lambda_B} = \frac{2\tilde{n}}{c\Delta\lambda_B} \tag{13}$$

where $\Delta\lambda_B$ represents the difference in the λ_B at the two ends of the grating ($=\lambda_{B(long)} - \lambda_{B(short)}$; $\lambda_{B(short)} \leq \lambda_0 \leq \lambda_{B(long)}$, λ_0 being the center wavelength). In this paper, D_g is set to be the total dispersion of SSMF ($\approx D_{SSMF}L_{SSMF}$), but with a negative value.

2.4 Signal detection and Q-factor estimation

A PIN photodetector is used to detect the received optical signal and convert it into an electrical form. The detected current is calculated as (Agrawal 1997):

$$i(t) = i_s(t) + i_T(t) + i_d + i_{sh}(t) \quad (14)$$

where $i_s(t) = RP_{in}(t)$ is the photodetector current, R is the receiver responsivity and $P_{in}(t)$ is the received optical power, $i_T(t)$ is a current fluctuation induced by thermal noise and calculated from the power spectral density, i_d is the dark current, and $i_{sh}(t) = q(i_s(t) + i_d)$ is the shot noise current whose noise distribution is assumed Gaussian.

The quality of the transmission system is characterized typically in terms of the eye diagram and the associated Q -factor of the received electrical signal. The Q -factor is calculated as (Agrawal 1997):

$$Q = \frac{|\mu_1 - \mu_0|}{\sigma_1 + \sigma_0} \quad (15)$$

where μ_i and σ_i with $i = "1" \text{ or } "0"$, are the average values and standard deviations of the sampled values, respectively. The greater the vertical difference between the average signal levels for "1" and "0", the more eye-opening and the higher the Q -factor, which indicates a lower bit error rate (BER). Therefore, the Q -factor is used to quantify the degree of vertical eye-opening (Agrawal 1997). According to ITU-T recommendations, BER is limited by 10^{-12} , which corresponds to $Q \approx 7$.

The commercial Optisystem software is used to simulate the above theoretical models of a 40-Gb/s fiber link. The numerical values of all used parameters related to the laser diode (quantum well InGaAsP-DFB), SSMF, NZ-DSF, DCF, FBG, and PIN photodetector of the proposed link and WDM system are given in Table 1 (Kashyap 1999; Hayee and Willner 1999; Agrawal 2002; Sato et al. 2005).

3 Results and discussions

3.1 Effects of linewidth enhancement factor and dispersion management methods on 40-Gb/s optical fiber link performance

The linewidth enhancement factor α is an important parameter that characterizes the frequency chirp of directly modulated high-speed LDs and hence controls the transmission bit rate and fiber length (Sato et al. 2005; Fouad et al. 2022). When chirped laser signals are transmitted over a dispersive fiber, the system performance is degraded. To reduce the dispersion effect of the fiber, dispersion management methods are often used (Krehlik 2006, 2007; Ahmed 2012). In this section, we investigate the effect of the α -parameter in the presence of dispersive SSMF and with the use of different dispersion management methods (NZ-DSF, DCF, and FBG) on the performance of 40-Gb/s directly-modulated optical fiber links at different transmission distances.

Figures 1a–d plot the variation of the Q -factor with the α -parameter when the modulated laser signals travel over SSMF, –NZ-DSF, +NZ-DSF, DCF with SSMF, and FBG with SSMF at different fiber lengths L of 5, 10, 25, 40 km, respectively. The figures illustrate that the increase in α from 1 to 10 causes a reduction in the modulated signal quality (i.e., the Q -factor decreases) regardless of the dispersion management method. This degradation in the quality is due to the increase of the transient chirp effect associated with the increase of α . This result agrees with the findings reported by (Fouad et al. 2022). The figures illustrate also that the increase in transmission length causes an additional degradation in the link performance. This indicates that the dispersion accumulated along the fiber

Table 1 The components of the proposed simulation models and their parameter values

Component	Parameter	Value
Laser diode	Wavelength, λ	1.55 μm
	Active layer volume, V	$3 \times 10^{-11} \text{ cm}^3$
	Group velocity, v_g	$8.33 \times 10^9 \text{ cm/s}$
	Quantum efficiency, η_o	0.255
	Differential gain coefficient, a_o	$9.9 \times 10^{-16} \text{ cm}^2$
	Carrier density at transparency, N_o	$1.23 \times 10^{18} \text{ cm}^{-3}$
	Linewidth enhancement factor, α	(1–10)
	Mode confinement factor, Γ	0.2
	Photon lifetime, τ_p	$1.69 \times 10^{-12} \text{ s}$
	Electron lifetime, τ_e	$776 \times 10^{-12} \text{ s}$
	Spontaneous emission factor, β	3×10^{-5}
	Gain compression coefficient, ϵ	$2.77 \times 10^{-17} \text{ cm}^3$
	Threshold current, I_{th}	9.8 mA
	Bias current, I_b	98 mA
	Modulation peak current, I_m	49 mA
SSMF	Attenuation coefficient, α_f	0.2 dB/km
	Dispersion, D_{SSMF}	+16.75 ps/nm/km
	Dispersion slope, S_{SSMF}	0.075 ps/nm ² /km
NZ-DSF	Attenuation coefficient, α_{NZ-DSF}	0.185 dB/km
	Dispersion, D_{NZ-DSF}	+4.5 and -7.5 ps/nm/km
	Dispersion slope, S_{NZ-DSF}	0.01 ps/nm ² /km
DCF	Attenuation coefficient, α_{DCF}	0.6 dB/km
	Dispersion, D_{DCF}	-82 ps/nm/km
FBG	Dispersion slope, S_{DCF}	0.35 ps/nm ² /km
	Center wavelength, λ_o	1.55 μm
	Core refractive index, \tilde{n}	1.45
PIN	Grating length, L_g	20 nm
	Chirp function	Linear
	Responsivity, R	1 A/W
PIN	Thermal noise, i_T	10–22 W/Hz
	Dark current, i_d	10 A

(which increases with the increase of transmission distance) is the main contributor to the increased effect of laser chirp as reported in (Krehlik 2007; Ahmed 2012). As a numerical example, without dispersion management, when SSMF is as short as $L_{SSMF}=5$ km, the Q -factor decreases from 4 to 0 when α increases from 1 to 6 (see Fig. 1a). When L_{SSMF} increases to 10 km, the Q -factor decreases from 3.5 to 0 when α increases from 1 to 4 (see Fig. 1b). The signals are completely degraded (Q -factor=0) when $L_{SSMF}=25$ and 40 km as shown in Fig. 1c and d, respectively. In all cases, the Q -factor is smaller than the minimum acceptable value (≥ 7), which indicates low link performance.

The use of dispersion management methods often improves the link performance with different levels. When SSMF is replaced by -NZ-DSF at $L_{-NZ-DSF}=5$ km, the Q -factor increases from 4 (unacceptable Q -factor) to 8.5 (acceptable Q -factor) when $\alpha=1$, respectively, as shown in Fig. 1a. The use of -NZ-DSF at lengths of 10 and 25 km also improves

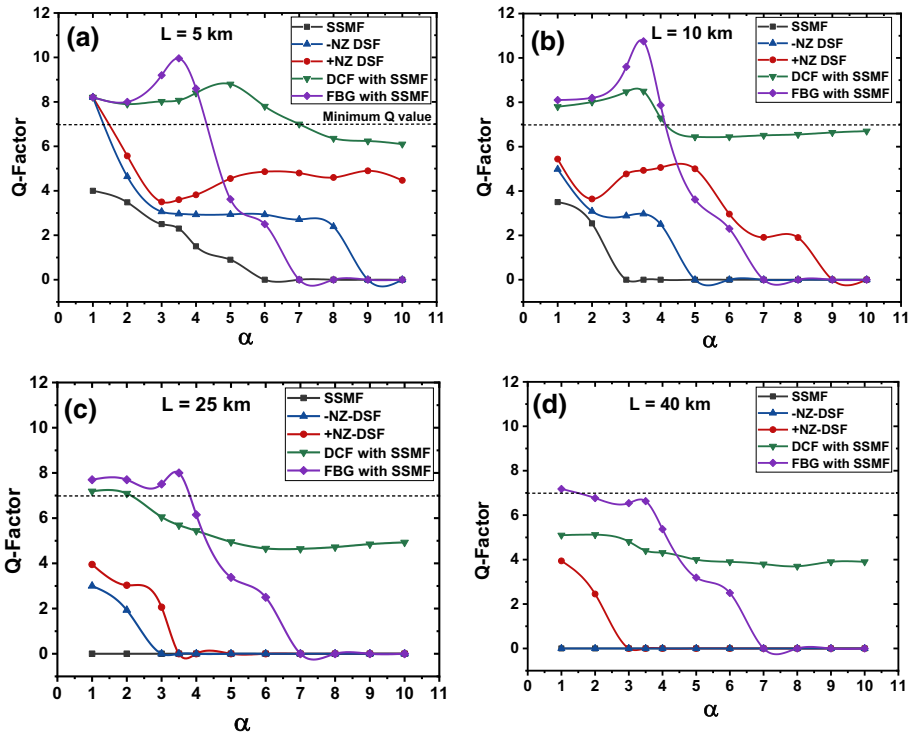


Fig. 1 Variation of Q -factor with linewidth enhancement factor α when 40-Gb/s modulated laser signals transmitted over SSMF, -NZ-DSF, +NZ-DSF, DCF with SSMF, and FBG with SSMF at different transmission lengths of **a** 5, **b** 10, **c** 25, and **d** 40 km

the Q -factor better than SSMF but remains smaller than the minimum acceptable value. When the transmission length reaches 40 km, the -NZ-DSF behaves like SSMF; the signals are completely deteriorated for the entire range of the α -factor, as shown in Fig. 1d. Replacing SSMF with +NZ-DSF almost gives the same behavior as -NZ-DSF in improving the link performance, but with slightly higher efficiency (i.e., it has larger Q -factor values than -NZ-DSF) over the entire values of α . The use of DCF or FBG with SSMF induces a significant improvement in the Q -factor values better than -NZ-DSF and +NZ-DSF, especially at smaller values of α and/or long fibers. Up to $\alpha=4$, the use of FBG with SSMF provides better performance of the fiber link (it becomes able to compensate for the dispersion of SSMF more) than the use of DCF with SSMF as shown in Fig. 1a–d, which agrees with the findings reported by (Meena and Gupta 2019). The use of FBG with SSMF is characterized by a peak for Q -the factor values at $\alpha=3.5$ when the transmission lengths L are 5, 10, and 25 km. Moreover, it maintains the link performance at long transmission distances such as 40 km when $\alpha=1$ (see Fig. 1d). Therefore, in such 40-Gb/s optical fiber links, the use of FBG with SSMF is recommended for reducing the effect of SSMF chromatic dispersion at rather small values of the α -parameter, and it is also suitable for long transmission distances.

Figure 2a and b plot variation of the Q -factor over a wide range of the transmission distance (0.5~40 km) under the effect of the SSMF dispersion and with the use of different

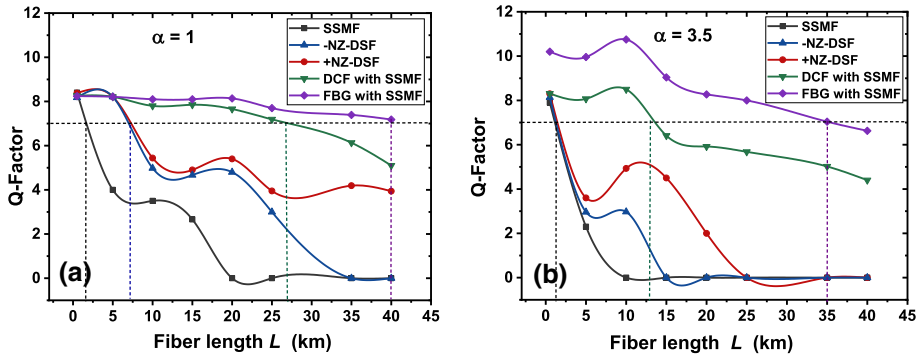


Fig. 2 Variation of Q -factor with the transmission fiber length when the modulated laser signals transmitted over SSMF, -NZ-DSF, +NZ-DSF, DCF with SSMF, and FBG with SSMF when **a** $\alpha = 1$, and **b** $\alpha = 3.5$

dispersion management methods at the two key values of $\alpha = 1$ and 3.5, respectively. The figures show that the Q -factor decreases with the increase of the SSMF length even when the dispersion management methods are used. The transmission distance is limited by the interaction of the laser chirp with the fiber dispersion as reported in (del Río Campos and Horche 2012; Fouad et al. 2022). The nonlinear interaction between overlapping pulses degrades the signal quality to a point where GVD compensation alone is ineffective for long-fiber links (Agrawal 2002). The ability of dispersion management to improve the 40-Gb/s link performance (or increases the transmission distance) is ordered as follows. The use of -NZ-DSF is the least effective method for managing the dispersion effect, followed by +NZ-DSF, then DCF with SSMF. The use of FBG with SSMF gives the best performance over the entire used fiber length. The maximum transmission length that corresponds to transmission free from error (i.e. $BER \approx 10^{-12}$ or Q -factor ≈ 7) for each dispersion management method is determined from the figures as follows. When $\alpha = 1$ (i.e., at weak laser chirp effect), the use of SSMF limits the transmission length to 1.6 km, while it is increased to 7.2, 26.5, and 40 km when using -NZ-DSF or +NZ-DSF, DCF with SSMF, and FBG with SSMF, respectively, as illustrated in Fig. 2a. Whereas when $\alpha = 3.5$ (i.e., at stronger laser chirp effect), the maximum transmission length reaches 1.2 km when using SSMF, -NZ-DSF, or +NZ-DSF, while it is increased to 13 and 35 km when using DCF with SSMF, and FBG with SSMF, respectively, as illustrated in Fig. 2b. The limitation of the fiber length with the increase of α is consistent with the reports in (Krehlik 2007; Ahmed 2012). From the above results, it is worth noting that the combination of FBG with SSMF outperforms the combination of DCF and SSMF in transmission quality. This is due to the extremely high negative dispersion of DCF induces some penalties such as nonlinear effects and insertion loss, particularly in long-distance communication systems (Willner et al. 2005; Gnanagurunathan and Rahman 2006). In contrast, FBG occupies smaller dimensions and has low nonlinear effects as well as low insertion loss, which results in better performance of the received signals and improves BER and Q -factor values. Therefore, the use of FBG with SSMF is recommended as a good solution that meets the needs of such high-speed links as reported by (Tan et al. 2009; Chaoui et al. 2015; Chakkour et al. 2017; Meena and Gupta 2019; Meena and Meena 2020).

The influence of dispersion management methods under different transmission lengths is investigated using the eye diagram analysis. Figure 3a and b display the evolution of the eye diagram of the received signals under the effect of SSMF dispersion and the four

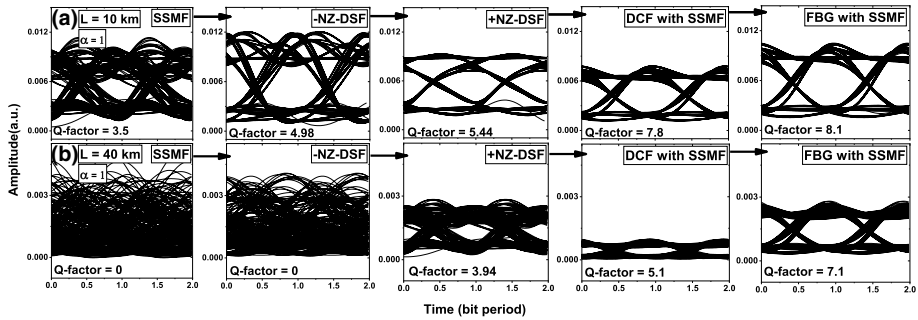


Fig. 3 Eye diagram evolution of the received signals at $\alpha=1$, when the modulated laser signals are transmitted over SSMF, $-NZ$ -DSF, $+NZ$ -DSF, DCF with SSMF, and FBG with SSMF at different transmission lengths of **a** $L=10$ and **b** $L=40$ km

different dispersion management methods ($-NZ$ -DSF, $+NZ$ -DSF, DCF with SSMF, and FBG with SSMF) at a constant value of $\alpha=1$ when the transmission length is $L=10$ and 40 km, respectively. Figure 3a shows that for SSMF with $L=10$ km, the eye pattern is partially closed with a small value of Q -factor= 3.5 , indicating low link performance. When SSMF is replaced by $-NZ$ -DSF or $+NZ$ -DSF, the eye is slightly improved, but it remains within the unacceptable Q -factor range ($=4.98$ or 5.44 , respectively). When DCF or FBG is used with SSMF, the eye diagram is well-opened with acceptable values of Q -factor= 7.8 or 8.1 , respectively (see Fig. 3a). When the transmission length is increased to 40 km, the degree of eye-opening decreases for all diagrams, and the Q -factor values reduce (see Fig. 3b). This indicates that the fiber dispersion has a significant effect on the performance of long fiber links and confirms the concept of dispersion-induced limitation on fiber length reported in (Ahmed 2012). Figure 3b reveals that the eye diagram is completely closed (Q -factor= 0) for SSMF and/or $-NZ$ -DSF over the long transmission distance of 40 km, whereas the use of $+NZ$ -DSF and DCF with SSMF improves the eye-opening but with unacceptable Q -factor values of 3.94 and 5.1 , respectively. The acceptable link performance at 40 km is achieved only when using FBG with SSMF with $\alpha=1$ as shown in Fig. 3b. These eye diagram investigations are consistent with the results in Fig. 2a.

To assess the contribution of α (or laser chirp) with the fiber dispersion in limiting the transmission distance, Fig. 4a and b plot the eye diagrams under the same conditions as Fig. 3a and b, but when α is increased to 3.5 . The figures reveal that the increase in α (which in turn induces an increase in the laser transient chirp) results in a significant increase in eye closure and thus a drop in the Q -factor values when compared to those of Fig. 3a and b, respectively. This is attributed to the increase in the transient chirping effect associated with enhanced overshoots in the transient regime of the laser (Fouad et al. 2022) in addition to the increased random fluctuations in the turn-on delay time (the time required for the carrier density to reach the threshold value) (del R o Campos et al. 2010). It is also worth noting that the thick horizontal borders of both the "1" and "0" levels that appear in the eye diagrams are due to laser and receiver noises. The shown bulges on the top of the eye diagram are due to the pseudo-random bit pattern effect that causes different paths of rising to level "1" or falling to level "0," depending on the history of the "0" bits preceding each "1" bit. The bit pattern effect stems from the fact that the bit slot in high-speed links, such as 40 -Gb/s, is shorter than the settling time of the laser relaxation oscillations (the

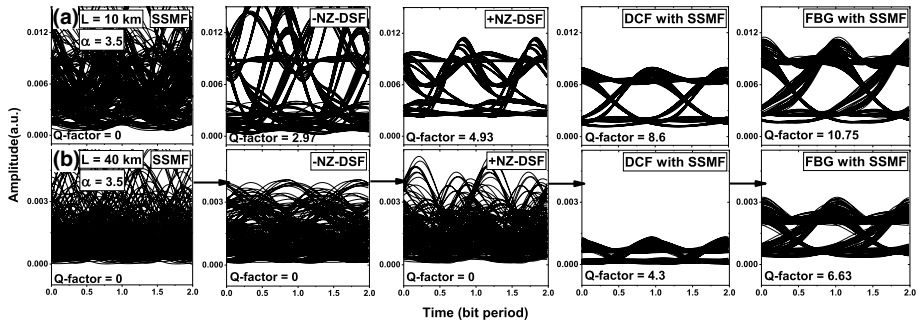


Fig. 4 Eye diagram evolution of the received signals at $\alpha=3.5$, when the modulated laser signals are transmitted over SSMF, -NZ-DSF, +NZ-DSF, DCF with SSMF, and FBG with SSMF at different transmission lengths of **a** $L=10$ and **b** $L=40$ km

time at which oscillations die out) (Ahmed et al. 2012, 2014). It is worth noting that the intrinsic laser parameters and the modulation parameters (such as bias current, modulation current, and modulation bit rate) given in Table 1, which control the initial pulses, are constant for all dispersion-management methods. However, the variation in pulse amplitude appearing in each method is attributed to the different attenuation coefficients of each method as listed in Table 1.

It can be concluded that the acceptable link performance for a transmission distance of 10 km when $\alpha=1$ is achieved by using DCF with SSMF or FBG with SSMF (see Fig. 3a), while for 40 km this is achieved only when using FBG with SSMF as shown in Fig. 3b. When α is increased to 3.5, the acceptable link performance for 10 km is achieved also by using DCF with SSMF or FBG with SSMF (see Fig. 4a), while the link performance is not acceptable when 40 km as shown in Fig. 4b. This indicates that the acceptable performance of 40-Gb/s optical fiber link decreases with the increase in α and/or transmission fiber length. Moreover, using FBG with SSMF is proven as the best-proposed dispersion management method for high-speed long-haul WDM optical communication systems, which agrees with the findings reported in (Meena and Gupta 2019; Meena and Meena 2020).

3.2 Performance of four-channel \times 40-Gb/s WDM transmission system using FBG with SSMF

In this section, we examine the effect of the linewidth enhancement factor α and transmission length on a dispersion-managed four-channel WDM system. Each channel corresponds to a 40-Gb/s directly-modulated optical link using FBG with SSMF for each channel as the recommended method to manage SSMF dispersion, as shown above. The channels are arranged as follows, Ch1, Ch2, Ch3, and Ch4 with laser wavelengths of 1531, 1551, 1571, and 1591 nm, respectively, as a coarse WDM system based on ITU-T Recommendation G.694.2 (Sector 2002). Figure 5a and b plot the variation of the Q -factor of each channel over a wide range of transmission lengths ($L=2\sim 40$ km) at the two values of α under investigation ($=1$ and 3.5 , respectively). The figures show that the performance of the WDM system reduces with the increase of the transmission length L . This reduction is small when $\alpha=1$, whereas it is large when $\alpha=3.5$. As a numerical example, when $\alpha=1$, the increase of the transmission length from $L=2$ to 40 km drops the Q -factor values of Ch4 from 8.3 to 5.2, respectively (see Fig. 5a), whereas the drop is from 10.7 to 2.8 when

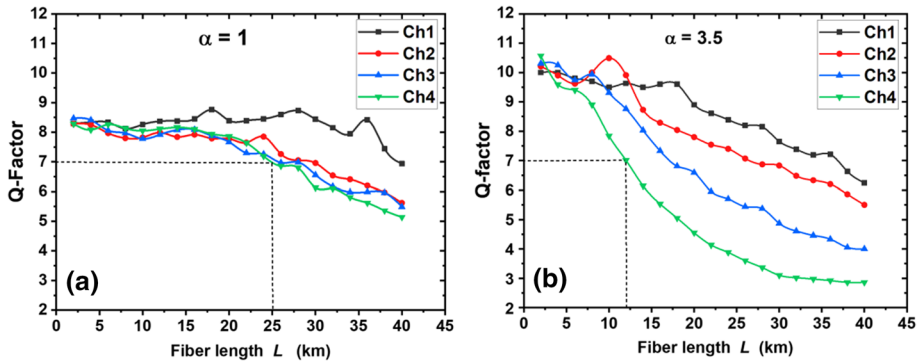


Fig. 5 Q -factor versus fiber length for a 4-channel \times 40-Gb/s—coarse WDM optical system using FBG with SSMF as a dispersion management method when **a** $\alpha = 1$ and **b** $\alpha = 3.5$

$\alpha = 3.5$ (see Fig. 5b). Moreover, when $\alpha = 1$, the difference in the performance between the channels is almost negligible along the transmission lengths (i.e. they have almost the same Q -factor values) except for Ch1. When $\alpha = 3.5$, the channels have a significant difference in the Q -factor values (~ 1.5), especially at long fibers. This is due to the effect of laser chirp, which increases when α increases. The maximum transmission length, which corresponds to error-free transmission, is determined by the minimum acceptable performance (i.e. Q -factor ≥ 7) for the worst channel. Therefore, the maximum transmission length when $\alpha = 1$ is 25 km, whereas it decreases to 12 km when $\alpha = 3.5$.

4 Conclusions

We presented a numerical simulation study on the effect of the laser linewidth enhancement factor α and potential methods for dispersion management on the performance of 40-Gb/s directly-modulated optical fiber links and WDM system. The dispersion management methods include the use of $-NZ$ -DSF, $+NZ$ -DSF, DCF, and FBG. The optimal α values and the best dispersion management method are predicted and applied to design and simulate a four-channel WDM system with different transmission lengths; each channel is a 40-Gb/s link. The performance of both the optical fiber link and the proposed WDM system is evaluated in terms of the eye diagram and Q -factor. The study is based on numerical integration of the rate equations of directly modulated LDs emitting $1.55 \mu\text{m}$ using NRZ pseudorandom bit streams and the nonlinear Schrodinger equation of wave propagation down the optical fiber. The obtained results can be summarized as follows:

1. The increase in the α -parameter and/or transmission length reduces the performance of both the 40-Gb/s optical link and the WDM system regardless of the applied method of dispersion management.
2. The use of $-NZ$ -DSF is the least effective method for managing the dispersion effect, followed by $+NZ$ -DSF, then DCF with SSMF, and FBG with SSMF.
3. When $\alpha = 1$, the use of SSMF limits the transmission length to 1.6 km, while the length increases to 7.2, 26.5, and 40 km when using $-NZ$ -DSF or $+NZ$ -DSF, DCF with SSMF, and FBG with SSMF, respectively. When $\alpha = 3.5$, the maximum transmission length is

- reduced to 1.2 km when using SSMF, -NZ-DSF, or +NZ-DSF, while it increases to 13 and 35 km when using DCF with SSMF, and FBG with SSMF, respectively.
4. The eye diagram opening is partially closed ($Q = 3.5$), indicating an unacceptable link performance (i.e. $Q < 7$) when the modulated laser signals at $\alpha = 1$ are transmitted over SSMF with a length of $L = 10$ km, while it is completely closed ($Q = 0$) when the laser signals are modulated at $\alpha = 3.5$. When DCF or FBG is used with SSMF, the eye diagram is well-opened with acceptable Q -factor values of 7.8 or 8.1, respectively when $\alpha = 1$ and 8.6 or 10.75, respectively when $\alpha = 3.5$. When the transmission length is increased to 40 km, the degree of eye-opening drops to unacceptable levels for all methods except when FBG is used with SSMF at $\alpha = 1$, which gives a Q -factor ≈ 7.1 .
 5. The use of FBG with SSMF provides the best performance, and hence it is a recommended method for the proposed WDM system, particularly over long distances.
 6. The performance of the WDM system is dropped with the increase of the transmission length. This reduction is small when $\alpha = 1$, but becomes large when $\alpha = 3.5$. The maximum transmission length for the proposed WDM system when $\alpha = 1$ is 25 km, whereas it is 12 km when $\alpha = 3.5$.

Acknowledgements Not applicable

Authors' contributions [AM]: Conceptualization, Formal analysis, Investigations, Writing—review & editing, Visualization. [NF]: Formal analysis, Investigations, Writing—original draft. [MA and TM]: Writing—review, Supervision.

Funding Open access funding provided by The Science, Technology & Innovation Funding Authority (STDF) in cooperation with The Egyptian Knowledge Bank (EKB). Not applicable.

Availability of data and materials Not applicable.

Declarations

Conflict of interest The authors declare that they have no known competing financial interests or personal relationships that could have appeared to influence the work reported in this paper.

Ethics approval and consent to participate Not applicable.

Consent for publication Not applicable.

Open Access This article is licensed under a Creative Commons Attribution 4.0 International License, which permits use, sharing, adaptation, distribution and reproduction in any medium or format, as long as you give appropriate credit to the original author(s) and the source, provide a link to the Creative Commons licence, and indicate if changes were made. The images or other third party material in this article are included in the article's Creative Commons licence, unless indicated otherwise in a credit line to the material. If material is not included in the article's Creative Commons licence and your intended use is not permitted by statutory regulation or exceeds the permitted use, you will need to obtain permission directly from the copyright holder. To view a copy of this licence, visit <http://creativecommons.org/licenses/by/4.0/>.

References

- Agrawal, G.P.: Intensity dependence of the linewidth enhancement factor and its implications for semiconductor lasers. *IEEE Photon. Technol. Lett.* **1**(8), 212–214 (1989). <https://doi.org/10.1109/68.36045>
- Agrawal, G.P.: *Nonlinear Fiber Optics*. Academic Press, San Diego (2001)
- Agrawal, G.P.: *Fiber-Optic Communication System*. Wiley-Interscience, New York (2002)
- Agrawal, G.P.: *Fiber-Optic Communication Systems*, vol. 222. Wiley, New York (2012)

- Agrawal, G.P., Bowden, C.M.: Concept of linewidth enhancement factor in semiconductor lasers: its usefulness and limitations. *IEEE Photon. Technol. Lett.* **5**(6), 640–642 (1993). <https://doi.org/10.1109/68.219695>
- Agrawal, G.P., Dutta, N.K.: *Long-wavelength semiconductor lasers*. New York: Van Nostrand Reinhold **1** 473, 338–339 (1986).
- Agrawal, G. P.: Chapter 2: Optical Fibers. *Fiber-Optic Communication Systems*. Wiley, New York (1997)
- Ahmed, M.: Modeling and simulation of dispersion-limited fiber communication systems employing directly modulated laser diodes. *Indian J. Phys.* **86**(11), 1013–1020 (2012). <https://doi.org/10.1007/s12648-012-0155-6>
- Ahmed, M., Mahmoud, S.W., Mahmoud, A.A.: Influence of pseudorandom bit format on the direct modulation performance of semiconductor lasers. *Pramana* **79**(6), 1443–1456 (2012). <https://doi.org/10.1007/s12043-012-0349-7>
- Ahmed, M., Mahmoud, S.W., Mahmoud, A.A.: Comparative study on modulation dynamic characteristics of laser diodes using RZ and NRZ bit formats. *Int. J. Numer. Model. Electron. Netw. Devices Fields* **27**(1), 138–152 (2014). <https://doi.org/10.1002/jnm.1905>
- Albeladi, F. T.: Performance of high speed laser diodes in optical fiber communication system. M.Sc. Thesis, King Abdulaziz University, Saudi Arabia (2013)
- Antoniades, N., Roudas, I., Ellinas, G., Amin, J.: Transport metropolitan optical networking: evolving trends in the architecture design and computer modeling. *J. Light. Technol.* **22**(11), 2653–2670 (2004). <https://doi.org/10.1109/JLT.2004.836776>
- Cartledge, J.C., Burley, G.S.: The effect of laser chirping on lightwave system performance. *J. Light. Technol.* **7**(3), 568–573 (1989). <https://doi.org/10.1109/50.16895>
- Chakkour, M., Aghzout, O., Ahmed, B.A., Chaoui, F., El Yakhloufi, M.: Chromatic dispersion compensation effect performance enhancements using FBG and EDFA-wavelength division multiplexing optical transmission system. *Int. J. Opt.* **2017**, 1–8 (2017). <https://doi.org/10.1155/2017/6428972>
- Chang, C.C., Weiner, A.M., Vengsarkar, A.M., Peckham, D.W.: Broadband fiber dispersion compensation for sub-100-fs pulses with a compression ratio of 300. *Opt. Lett.* **21**(15), 1141–1143 (1996). <https://doi.org/10.1364/OL.21.001141>
- Chaoui, F., Hajaji, A., Aghzout, O., Chakkour, M., Elyakhloufi, M.: Chirped Bragg grating dispersion compensation in dense wavelength division multiplexing optical long-haul networks. *Int. J. Microw. Opt. Technol.* **10**(5), 363–370 (2015)
- Chow, W.W., Depatie, D.: Carrier-induced refractive-index change in quantum-well lasers. *Opt. Lett.* **13**(4), 303–305 (1988). <https://doi.org/10.1364/OL.13.000303>
- del Río Campos, C., Horche, P.R., Martín-Minguez, A.: Analysis of linewidth and extinction ratio in directly modulated lasers for performance optimization in 10 Gbit/s CWDM systems. *Opt. Commun.* **283**(15), 3058–3066 (2010). <https://doi.org/10.1016/j.optcom.2010.03.066>
- del Río Campos, C., Horche, P. R.: Effects of Dispersion Fiber on CWDM Directly Modulated System Performance, *IntechOpen*, pp. 55–76 (2012)
- del Río Campos, C., Horche, P. R., Minguez, A. M.: Interaction of semiconductor laser chirp with fiber dispersion: Impact on WDM directly modulated system performance. In: *Proceedings of the 4th International Conference on Advances in Circuits, Electronics and Micro-electronics (CENICS)*, pp. 17–22 (2011)
- Duan, G.H., Gallion, P., Debarge, G.: Analysis of the phase-amplitude coupling factor and spectral linewidth of distributed feedback and composite-cavity semiconductor lasers. *IEEE J. Quantum Electron.* **26**(1), 32–44 (1990). <https://doi.org/10.1109/3.44914>
- Ellinas, G., Roudas, I.: Modeling, simulation, design and engineering of wdm systems and networks: an introduction. In: *WDM Systems and Networks*, pp 1–10 (2012). https://doi.org/10.1007/978-1-4614-1093-5_1
- Forsythe, G. E.: *Computer methods for mathematical computations*. Prentice-Hall Series in Automatic Computation (1977)
- Fouad, N., Mohamed, T., Mahmoud, A.: Impact of linewidth enhancement factor and gain suppression on chirp characteristics of high-speed laser diode and performance of 40 Gbps optical fiber links. *Appl. Phys. B* **128**(3), 1–11 (2022). <https://doi.org/10.1007/s00340-022-07771-5>
- Gnanagurunathan, G., Rahman, F. A.: Comparing FBG and DCF as dispersion in the long haul narrowband WDM systems. In: 2006 IFIP International Conference on Wireless and Optical Communications Networks (pp. 4-pp). *IEEE April* (2006) <https://doi.org/10.1109/WOCN.2006.1666665>
- Grüner-Nielsen, L., Knudsen, S.N., Edvold, B., Veng, T., Magnussen, D., Larsen, C.C., Damsgaard, H.: Dispersion compensating fibers. *Opt. Fiber Technol.* **6**(2), 164–180 (2000). <https://doi.org/10.1006/ofte.1999.0324>

- Harboe, P.B., da Silva, E., Souza, J.R.: Analysis of FWM penalties in DWDM systems based on G. 652, G. 653, and G. 655 optical fibers. *Int. J. Electr. Comput. Eng.* **2**(12), 2674–2680 (2008). <https://doi.org/10.5281/zenodo.1333622>
- Hayee, M.I., Willner, A.E.: NRZ versus RZ in 10–40-Gb/s dispersion-managed WDM transmission systems. *IEEE Photon. Technol. Lett.* **11**(8), 991–993 (1999). <https://doi.org/10.1109/68.775323>
- Henry, C.: Theory of the linewidth of semiconductor lasers. *IEEE J. Quantum Electron.* **18**(2), 259–264 (1982). <https://doi.org/10.1109/JQE.1982.1071522>
- Ismail, M.M., Othman, M.A., Zakaria, Z., Misran, M.H., Said, M.M., Sulaiman, H.A., et al.: EDFA-WDM optical network design system. *Procedia Eng.* **53**, 294–302 (2013). <https://doi.org/10.1016/j.proeng.2013.02.039>
- ITU-T draft recommendation G. 693, Optical Interfaces for Intra-Office Systems (2001).
- Kashyap, R.: *Fiber Bragg Gratings*. Academic Press, San Diego (1999)
- Kaur, M., Sarangal, H., Bagga, P.: Dispersion compensation with dispersion compensating fibers (DCF). *Int. J. Adv. Res. Comput. Commun. Eng.* **4**(2), 354–356 (2015). <https://doi.org/10.17148/IJARCCCE.2015.4280>
- Koch, T.L., Bowers, J.E.: Nature of wavelength chirping in directly modulated semiconductor lasers. *Electron. Lett.* **20**(25), 1038–1040 (1984). <https://doi.org/10.1049/el:19840709>
- Krehlik, P.: Characterization of semiconductor laser frequency chirp based on signal distortion in dispersive optical fiber. *Opto-Electron. Rev.* **14**(2), 119–124 (2006). <https://doi.org/10.2478/s11772-006-0015-z>
- Krehlik, P.: Directly modulated lasers in negative dispersion fiber links. *Opto-Electron. Rev.* **15**(2), 71–77 (2007). <https://doi.org/10.2478/s11772-007-0002-z>
- Kumano, N., Mukasa, K., Sakano, M., Moridaira, H.: Development of a non-zero dispersion-shifted fiber with ultra-low dispersion slope. *Furukawa Rev.* **22**(1), 1–6 (2002)
- Liu, J., Lam, Y.L., Chan, Y.C., Zhou, Y., Yao, J.: Fabrication of high-performance dispersion compensating fiber by plasma chemical vapor deposition. *Fiber Integr. Opt.* **18**(2), 63–67 (1999). <https://doi.org/10.1080/014680399244703>
- Lu, H.H.: Performance comparison between DCF and RDF dispersion compensation in fiber optical CATV systems. *IEEE Trans. Broadcast.* **48**(4), 370–373 (2002). <https://doi.org/10.1109/TBC.2002.805635>
- Meena, D., Meena, M. L.: Design and analysis of novel dispersion compensating model with chirp fiber bragg grating for long-haul transmission system. In: *Optical and Wireless Technologies*. Springer, pp. 29–36 (2020). https://doi.org/10.1007/978-981-13-6159-3_4
- Meena, M.L., Gupta, R.K.: Design and comparative performance evaluation of chirped FBG dispersion compensation with DCF technique for DWDM optical transmission systems. *Optik* **188**, 212–224 (2019). <https://doi.org/10.1016/j.ijleo.2019.05.056>
- Mohammadi, S.O., Mozaffari, S., Shahidi, M.M.: Simulation of a transmission system to compensate dispersion in an optical fiber by chirp gratings. *Int. J. Phys. Sci.* **6**(32), 7354–7360 (2011). <https://doi.org/10.5897/IJPS11.1504>
- Mohammed, N.A., Solaiman, M., Aly, M.H.: Design and performance evaluation of a dispersion compensation unit using several chirping functions in a tanh apodized FBG and comparison with dispersion compensation fiber. *Appl. Opt.* **53**(29), H239–H247 (2014). <https://doi.org/10.1364/AO.53.00H239>
- Nagarajan, R., Ishikawa, M., Fukushima, T., Geels, R.S., Bowers, J.E.: High speed quantum-well lasers and carrier transport effects. *IEEE J. Quantum Electron.* **28**(10), 1990–2008 (1992). <https://doi.org/10.1109/3.159508>
- Olofsson, L., Brown, T.G.: The influence of resonator structure on the linewidth enhancement factor of semiconductor lasers. *IEEE J. Quantum Electron.* **28**(6), 1450–1458 (1992). <https://doi.org/10.1109/3.135297>
- Osinski, M., Buus, J.: Linewidth broadening factor in semiconductor lasers—an overview. *IEEE J. Quantum Electron.* **23**(1), 9–29 (1987). <https://doi.org/10.1109/JQE.1987.1073204>
- Othonos, A., Kalli, K., Pureur, D., Mugnier, A.: *Fibre bragg gratings*. In: *Wavelength Filters in Fibre Optics*, pp 189–269. Springer, Berlin, Heidelberg (2006)
- Pande, K., Pal, B.P.: Design optimization of a dual-core dispersion-compensating fiber with a high figure of merit and a large effective area for dense wavelength-division multiplexed transmission through standard G 655 fibers. *Appl. Opt.* **42**(19), 3785–3791 (2003). <https://doi.org/10.1364/AO.42.003785>
- Peral, E., Marshall, W.K., Yariv, A.: Precise measurement of semiconductor laser chirp using effect of propagation in dispersive fiber and application to simulation of transmission through fiber gratings. *J. Light. Technol.* **16**(10), 1874–1880 (1998). <https://doi.org/10.1109/50.721075>
- Potasek, M.J., Agrawal, G.P.: Self-amplitude-modulation of optical pulses in nonlinear dispersive fibers. *Phys. Rev. A* **36**(8), 3862 (1987). <https://doi.org/10.1103/PhysRevA.36.3862>

- Priya, R., Sivanantharaja, A., Selvendran, S.: Performance analysis of optimized non-zero dispersion shifted fiber without amplification and without dispersion compensation for wavelength division multiplexing optical networks. *Opt. Appl.* **45**(4), 473–490 (2015). <https://doi.org/10.5277/oa150404>
- Recommendation ITU-T G.655 "Characteristics of a non-zero dispersion-shifted single-mode optical fiber and cable (2009)
- Sato, K., Kuwahara, S., Miyamoto, Y.: Chirp characteristics of 40-Gb/s directly modulated distributed-feedback laser diodes. *J. Light. Technol.* **23**(11), 3790–3797 (2005). <https://doi.org/10.1109/JLT.2005.857753>
- Sector, I. T. S.: Spectral grids for WDM applications: CWDM wavelength grid. ITU-T Recommendation G.694.2 (2002)
- Sinkin, O.V., Holzlöhner, R., Zweck, J., Menyuk, C.R.: Optimization of the split-step Fourier method in modeling optical-fiber communications systems. *J. Light. Technol.* **21**(1), 61 (2003). <https://doi.org/10.1109/JLT.2003.808628>
- Tan, Z., Wang, Y., Ren, W., Liu, Y., Li, B., Ning, T., Jian, S.: Transmission system over 3000 km with dispersion compensated by chirped fiber Bragg gratings. *Optik* **120**(1), 9–13 (2009). <https://doi.org/10.1016/j.ijleo.2007.01.018>
- Tomkos, I., Chowdhury, D., Conradi, J., Culverhouse, D., Enns, K., Giroux, C., et al.: Demonstration of negative dispersion fibers for DWDM metropolitan area networks. *IEEE J. Sel. Top. Quantum Electron.* **7**(3), 439–460 (2001a). <https://doi.org/10.1109/2944.962268>
- Tomkos, I., Roudas, I., Hesse, R., Antoniadis, N., Boskovic, A., Vodhanel, R.: Extraction of laser rate equations parameters for representative simulations of metropolitan-area transmission systems and networks. *Opt. Commun.* **194**(1–3), 109–129 (2001b). [https://doi.org/10.1016/S0030-4018\(01\)01230-5](https://doi.org/10.1016/S0030-4018(01)01230-5)
- Tucker, R.S.: High-speed modulation of semiconductor lasers. *IEEE Trans. Electron Devices.* **32**(12), 2572–2584 (1985). <https://doi.org/10.1109/T-ED.1985.22387>
- Wang, G., Nagarajan, R., Tauber, D., Bowers, J.: Reduction of damping in high-speed semiconductor lasers. *IEEE Photon. Technol. Lett.* **5**(6), 642–645 (1993). <https://doi.org/10.1109/68.219696>
- Westbrook, L.D., Adams, M.J.: Explicit approximations for the linewidth-enhancement factor in quantum-well lasers. *IEEE Proc. J. (Optoelectron.)* **135**(3), 223–225 (1988)
- Willner, A.E., Song, Y.W., McGeehan, J., Pan, Z., Hoanca, B.: Dispersion Management, *Encyclopedia of Modern Optics*, pp. 353–365. Elsevier, Amsterdam (2005). <https://doi.org/10.1016/B0-12-369395-0/00675-8>
- Yousuf, A.: Investigation on chirping induced performance degradation in single mode directly modulated 1.55 μm DFB laser. *J. Opt. Commun.* **40**(1), 31–36 (2019). <https://doi.org/10.1515/joc-2017-0015>
- Yousuf, A., Najeeb-ud-din, H.: Effect of gain compression above and below threshold on the chirp characteristics of 1.55 μm distributed feedback laser. *Opt. Rev.* **23**(6), 897–906 (2016). <https://doi.org/10.1007/s10043-016-0268-9>
- Zhang, K., Zhuge, Q., Xin, H., Hu, W., Plant, D.V.: Performance comparison of DML, EML and MZM in dispersion-unmanaged short reach transmissions with digital signal processing. *Opt. Express* **26**(26), 34288–34304 (2018). <https://doi.org/10.1364/OE.26.034288>